Original Article

Open Access

Check for updates

Supporting Information: Imaging Inter and Intra-particle Features in Crystalline Cathode Materials for Li-Ion Batteries using Nano-focused Beam Techniques at 4^{th} Generation Synchrotron Sources

Mattia Colalongo*[1,2], Nikita Vostrov*[1], Isaac Martens[1], Edoardo Zatterin[1], Marie-Ingrid Richard[1], Francois Cadiou[1], Quentin Jacquet[3], Jakub Drnec[1], Steven J. Leake[1], Tanja Kallio[2], Xiaobo Zhu[4], Sandrine Lyonnard[3], Tobias Schulli[1]

[1]European Synchrotron Radiation Facility, 71 Avenue des Martyrs, Grenoble 38000, France
[2]Department of Chemistry and Material Science, School of Chemical Engineering, Aalto University, Kemistintie 1, Espoo 02150, Finland
[3]Univ. Grenoble Alpes, CEA, CNRS, Grenoble INP, IRIG, SyMMES, 38000 Grenoble, France
[4]College of Materials Science and Engineering, Changsha University of Science and Technology, Changsha 410114, China

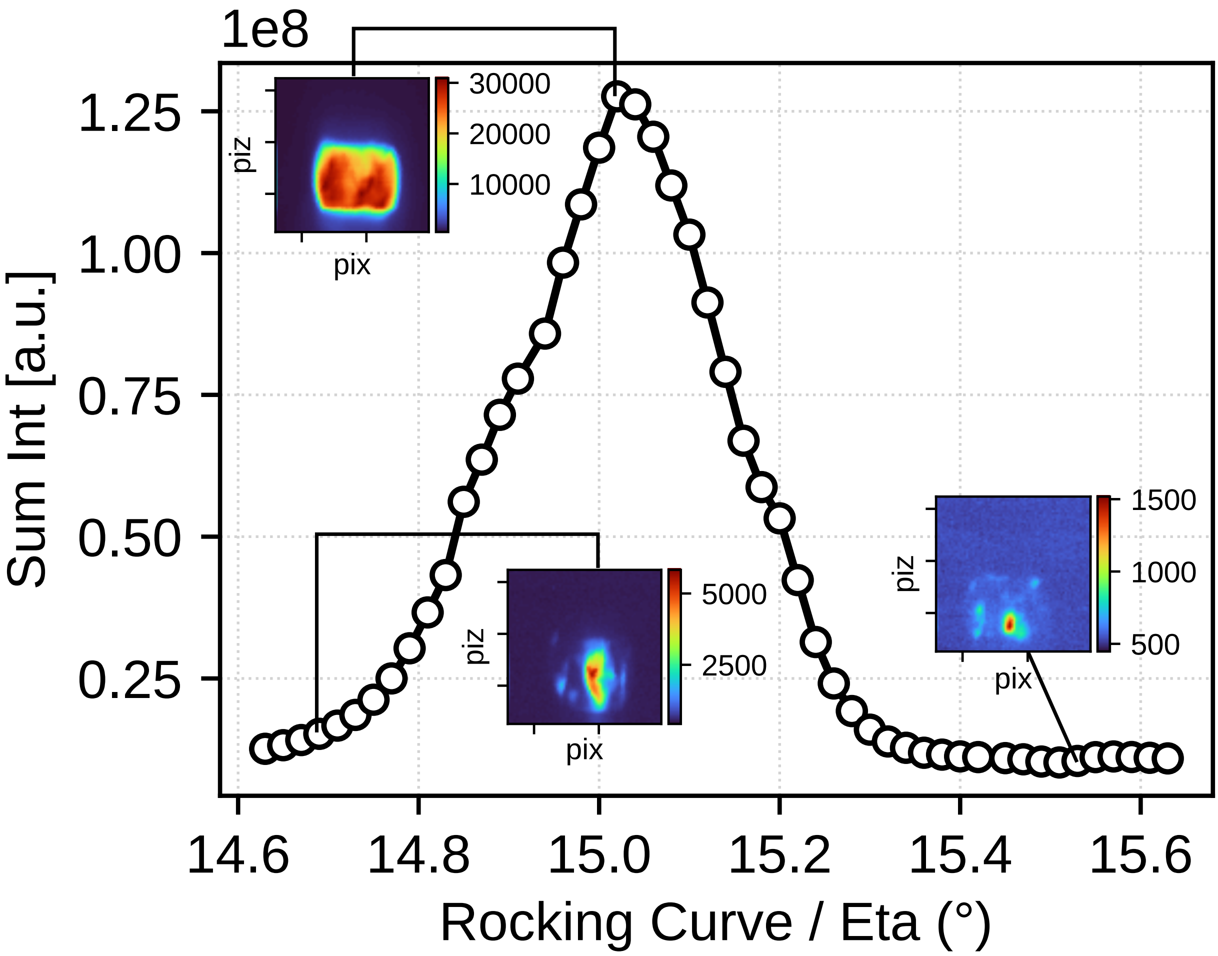

Figure S1. Rocking curve of a single crystal to collect the Bragg peak volume in reciprocal space. In each different *Eta* scan point we XY raster the particle. Every single XY scan position will contain a 2D information in Q_y and Q_z. Merging all the eta scans we finally retrieve the Q_x, Q_y and Q_z information of each XY position.

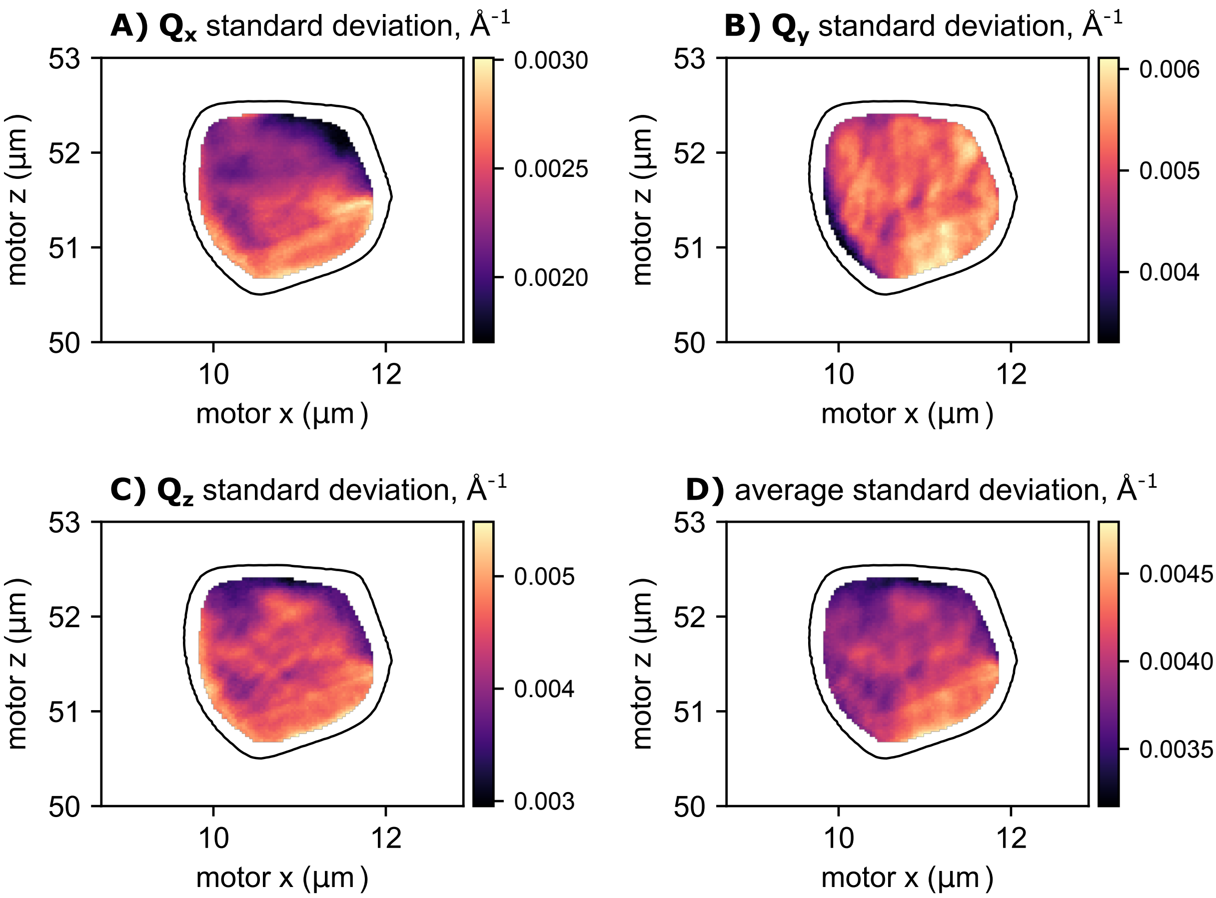

Figure S2. Standard deviation maps for Particle 1 obtained from fitting the diffraction peak of the particle in all three reciprocal space directions. A and B represent the widths of the peak (at each position of the real space map) along Q_x and Q_y which corresponds to the lattice misorientation heterogeneity and along Q_z (C) which indicates the local strain (d-spacing variation). (D) presents an average standard deviation across all three axes.

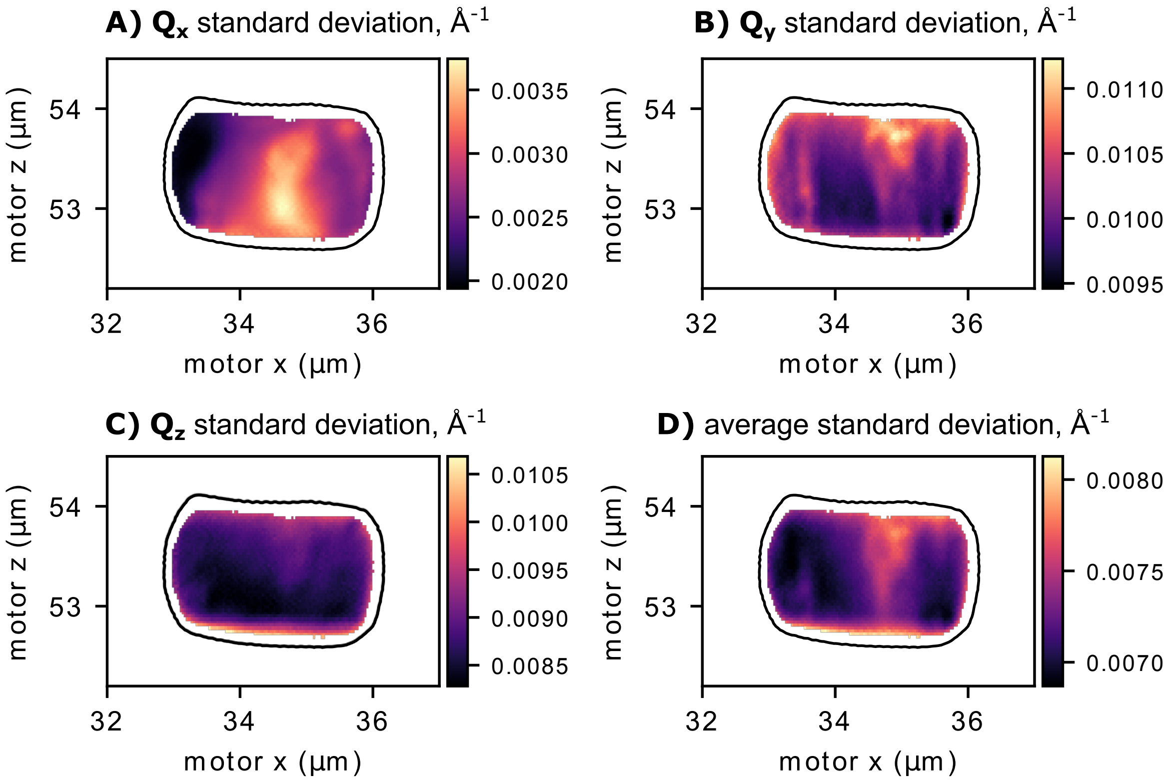

Figure S3. Standard deviation maps for Particle 2 obtained from fitting the diffraction peak of the particle in all three reciprocal space directions. A and B represent the widths of the peak (at each position of the real space map) along Q_x and Q_y which corresponds to the lattice misorientation heterogeneity and along Q_z (C) which indicates the local strain (d-spacing variation). (D) presents an average standard deviation across all three axes.

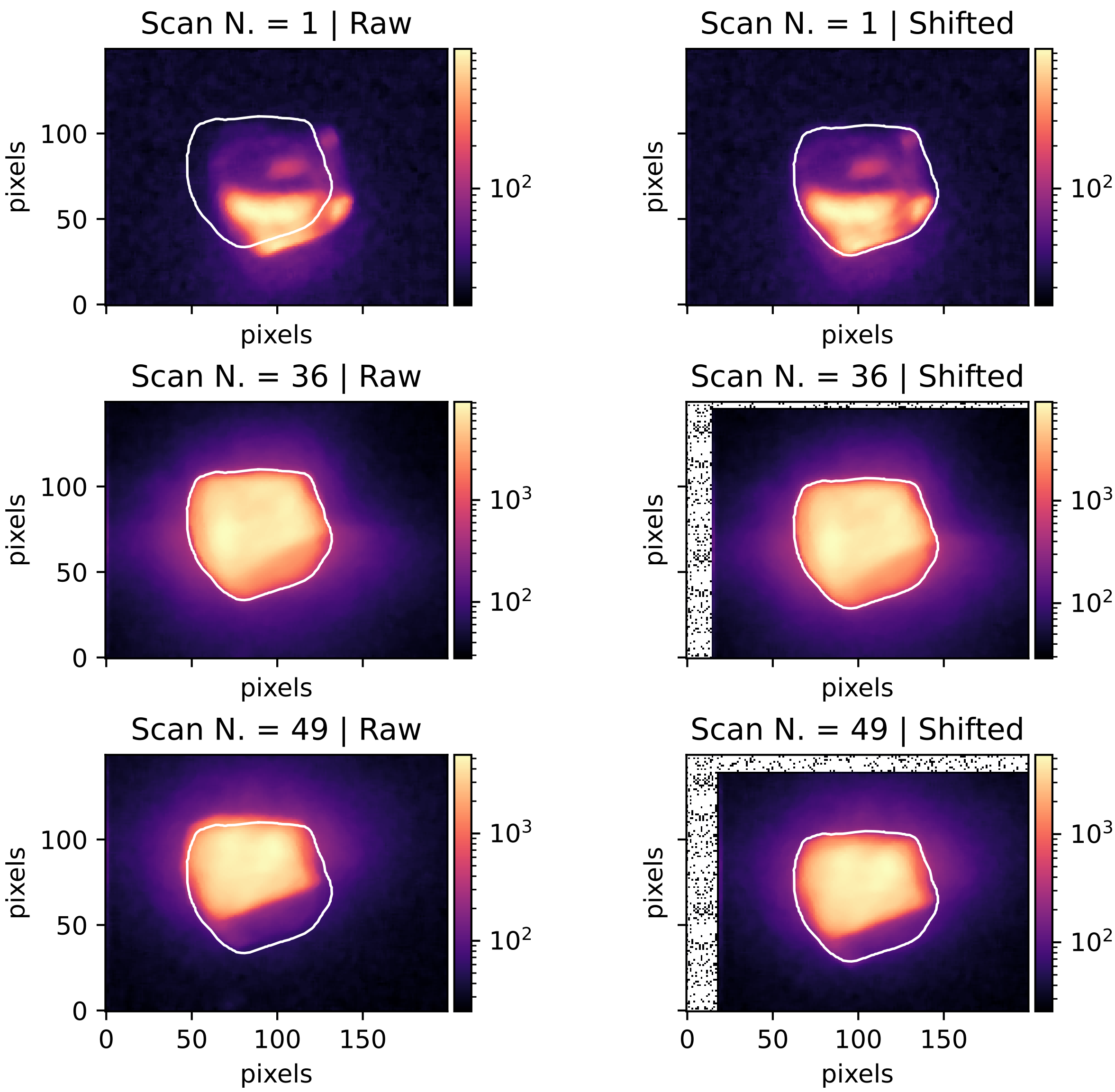

Figure S4. Linear Shift Correction applied to each scan of the rocking curve to compensate the small particle drift observed due to a center of rotation (CoR) misalignment.

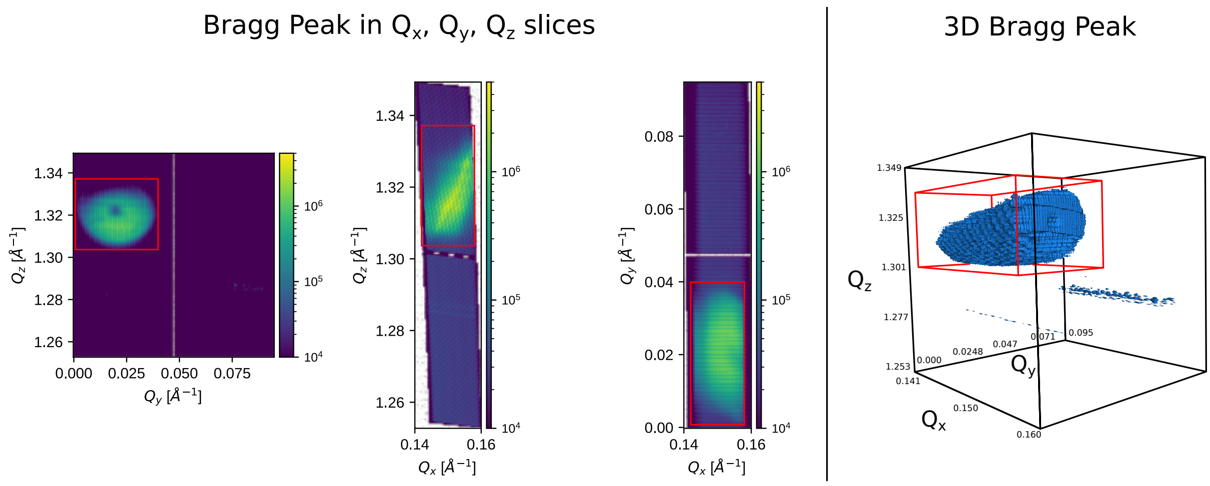

Figure S5. The selected region of interest in reciprocal space is defined by the red box in Qx, Qy and Qz, around the Bragg peak. On the right, the whole sampled 3D Bragg peak obtained after the full rocking curve.

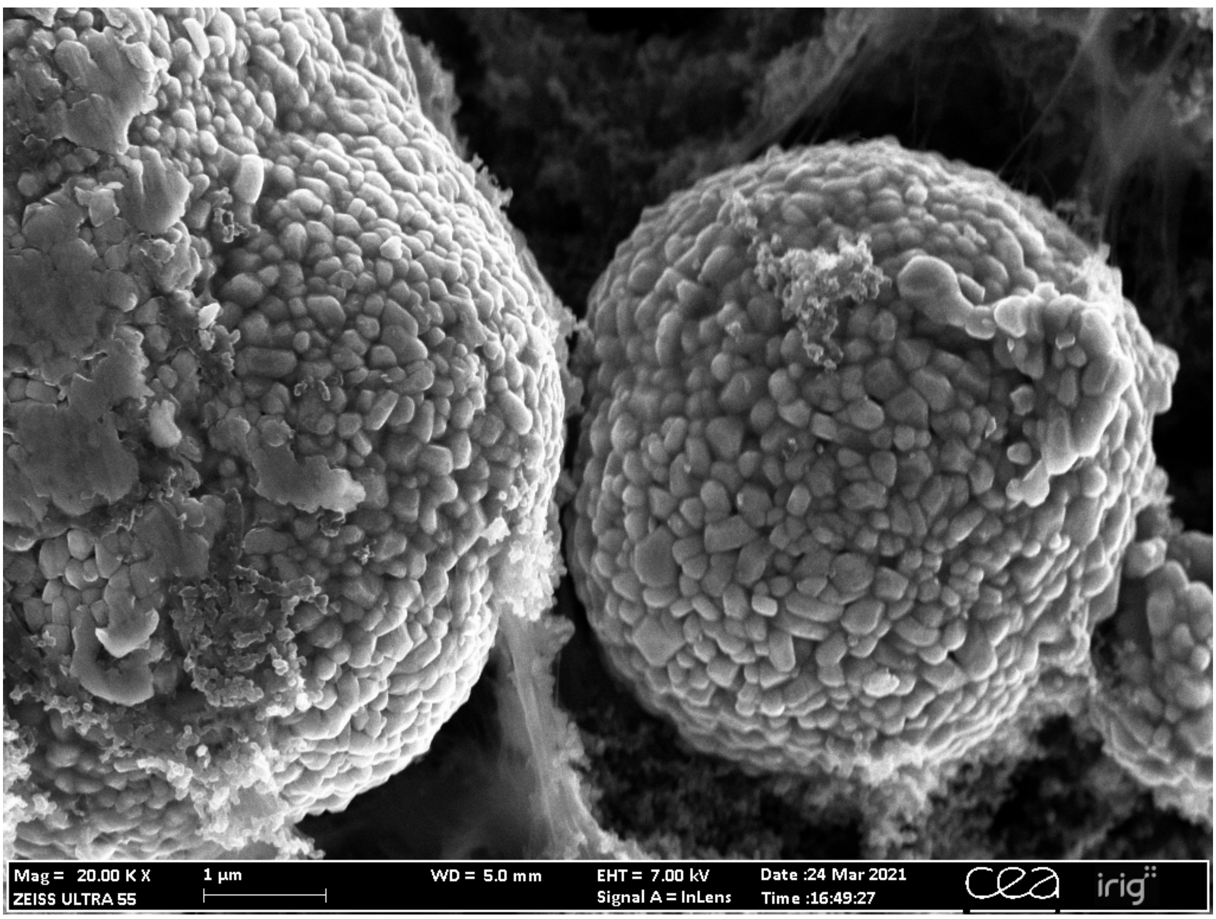

Figure S6. Scanning Electron Microscopy (SEM) of the LNO sample

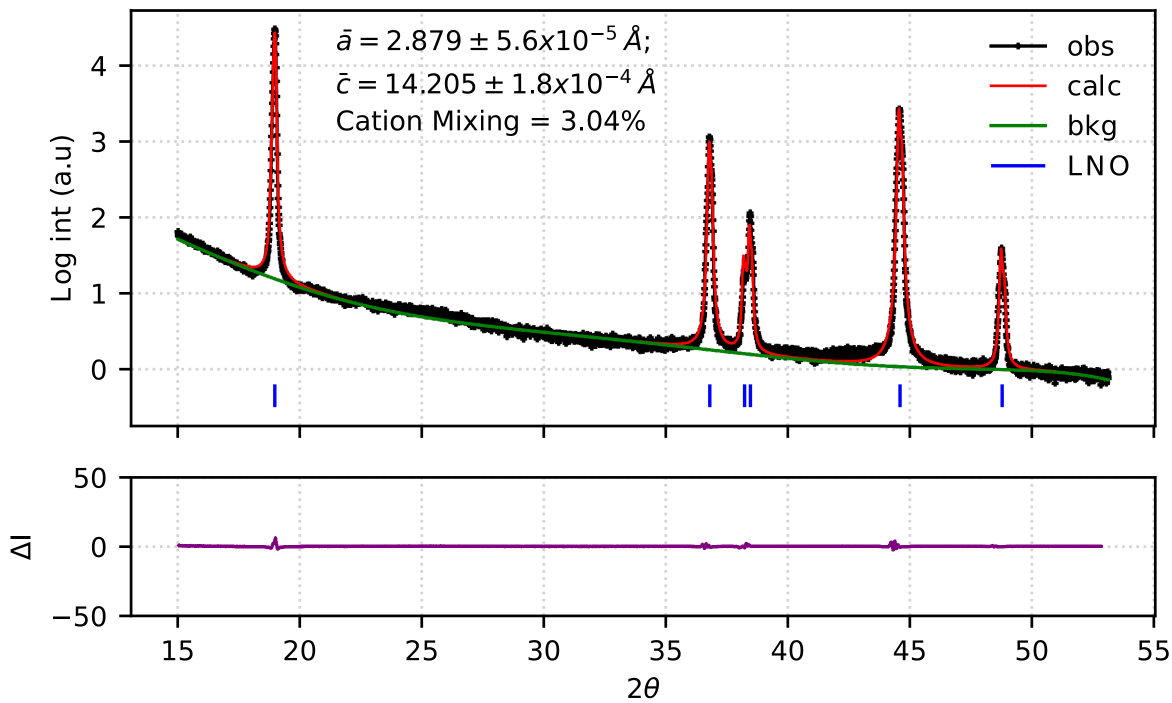

Figure S7. Powder diffraction Refinement of $LiNiO_2$. CIF file from ICSD-#104726.

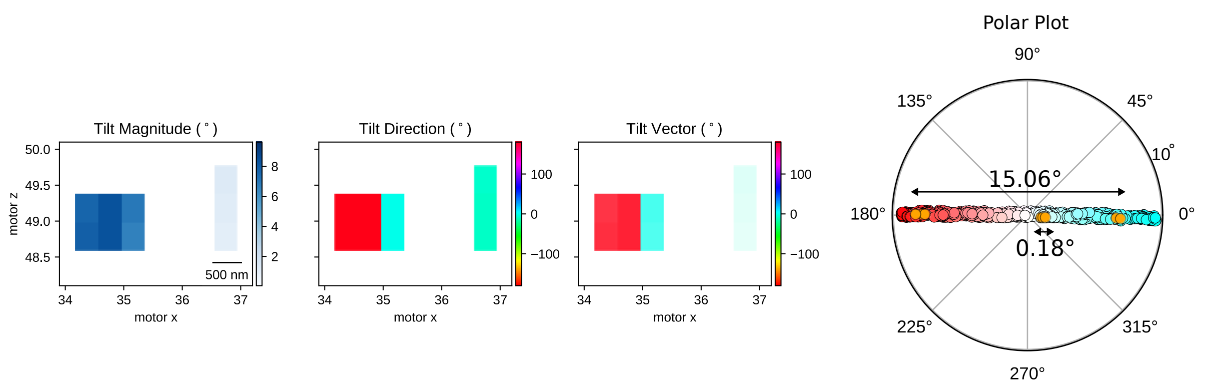

Figure S8. From left to right, Tilt Magnitude, Tilt Direction, Tilt Vector (Magnitude · Direction) and Polar Plot figures of the zoomed in portion of the full 40x40 μm map of the LNO sample. In the polar plot, in orange are represented the position of the map pixels compared to the whole 40x40 μm map. The maximum tilt extension is measured for the cluster of particle on the left ($\sim 15.06°$) and and the cluster of particles on the right ($\sim 0.18°$)

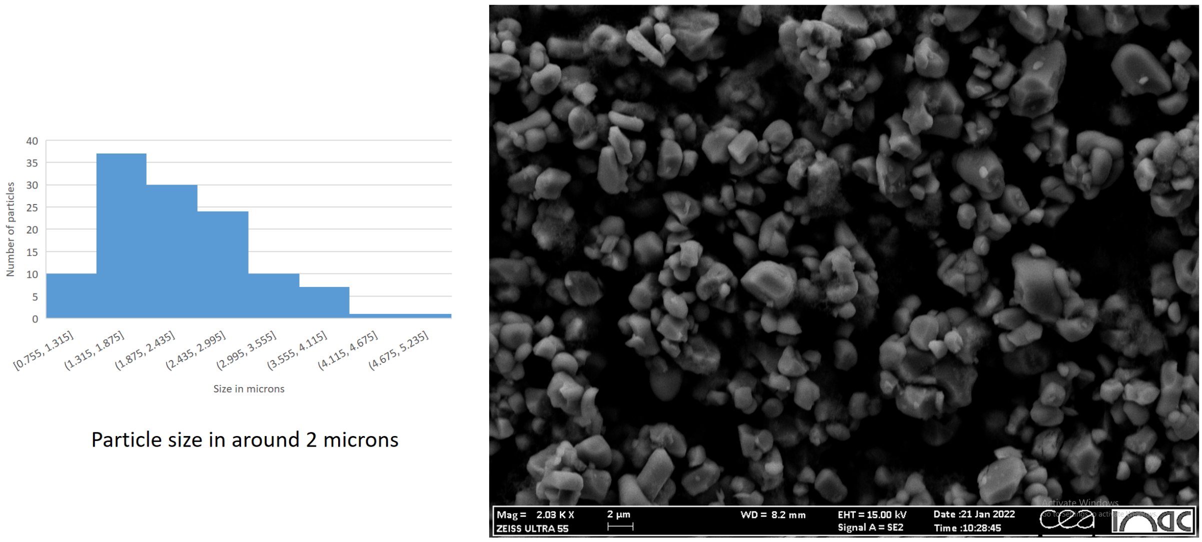

Figure S9. Particle Size distribution on the left, Scanning Electron Microscopy (SEM) of the SC-NMC622 sample on the right

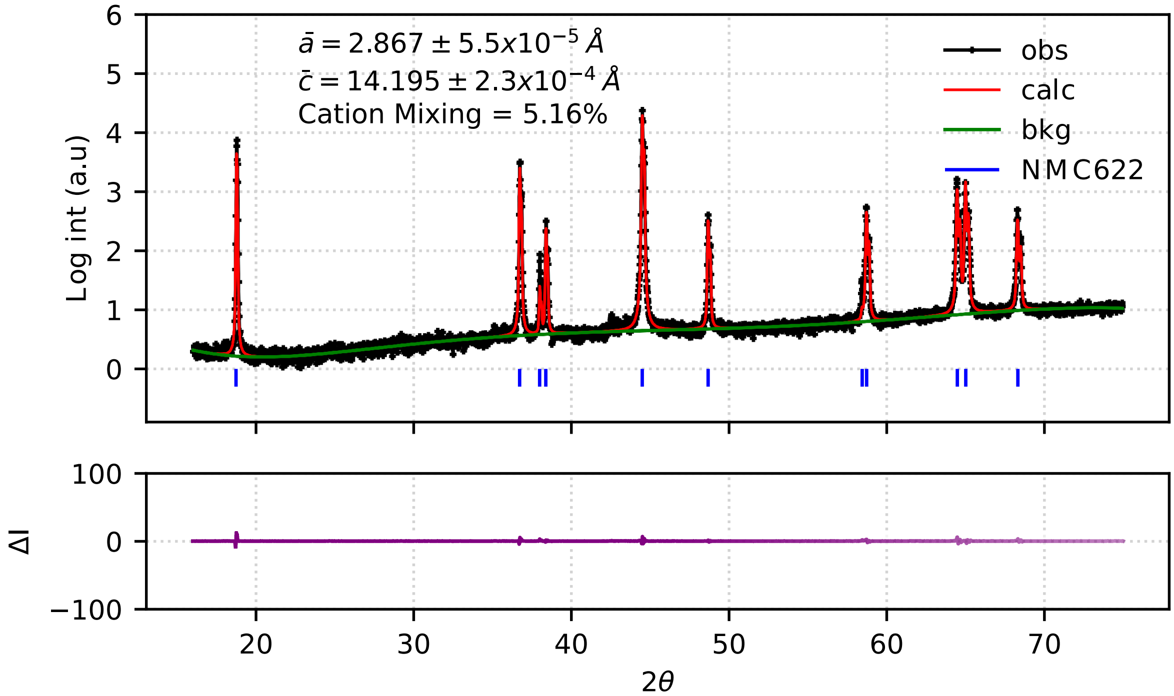

Figure S10. Powder diffraction Refinement of $LiNi_{0.6}Mn_{0.2}Co_{0.2}O_2$. CIF file from ICSD-#47972.

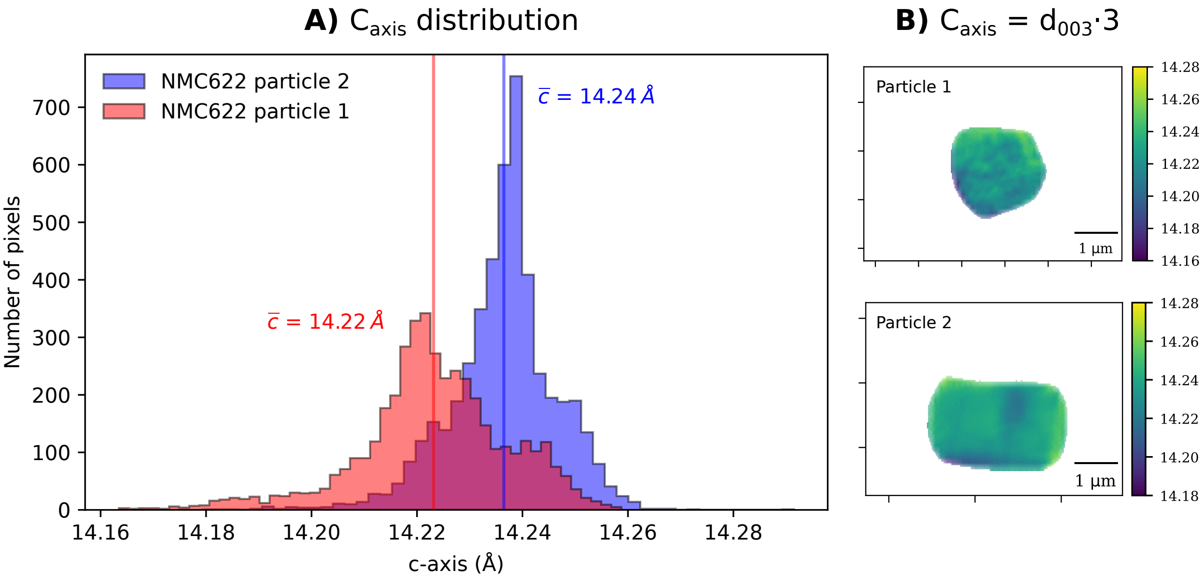

Figure S11. A) c-axis distribution per number of pixels for SC-NMC622 particle 1 and 2. B) 2D map c-axis distribution of the two measured particles. c-axis map is retrieved from the d-spacing map values times 3 as the hkl reflection involved is the 003